

## MINIATURIZED DUAL-BAND MATCHING TECHNIQUE BASED ON COUPLED-LINE TRANSFORMER FOR DUAL-BAND POWER AMPLIFIERS DESIGN

S. Li<sup>\*</sup>, B. H. Tang, Y. A. Liu, S. L. Li, C. P. Yu, and Y. L. Wu

School of Electronic Engineering, Beijing University of Posts and Telecommunications, Beijing, China

**Abstract**—This study presents a novel miniaturized dual-band coupled-line impedance transformer. This dual-band matching technique uses the characteristics of coupled-line and dual-band stubs to realize matching arbitrary complex impedance to arbitrary complex impedance at two arbitrary uncorrelated frequencies. Especially, it satisfies the demand of dual-band matching at two relatively closed operating frequencies ( $n = f_2/f_1 \leq 1.2$ ), and occupy a very small circuit area with inherent DC-Block function. The proposed synthesis approach is validated by the design and fabrication of a 30 W gallium nitride (GaN)-based class-AB power amplifier (PA) for GSM and WCDMA at 1800 MHz and 2140 MHz. The PA's output matching network based on the proposed structure can accurately match  $50\ \Omega$  to the ideal load impedances of the transistor at two designed frequency simultaneously and has 20% and 15% bandwidth for which the reflection coefficient magnitudes are less than 0.1, respectively.

### 1. INTRODUCTION

Nowadays, the requirement of dual-band operation for RF system is obviously increased with the trend of multiband applications in new technologies of wireless communication systems. For composing compact and low-cost multiband systems, multiband components and circuits are needed. The power amplifiers are the key part in the transmitter for mobile communication systems.

To achieve practical structures for this kind of circuits, a number of dual-band matching methods have been published [1–14]. Orfanidis

---

*Received 20 July 2012, Accepted 29 August 2012, Scheduled 9 September 2012*

\* Corresponding author: Shun Li (libukun@gmail.com).

presented dual-band transformers with Chebyshev response in [1]. Monzon proposed a small two-section transformer to deal with any two uncorrelated frequencies [2]. Wu et al. extended a two-section transformer to deal with a load of equal complex impedance at two frequencies [3]. Liu et al. presented a dual-band transformer using a three-section transmission line [4]. A compact Pi-structure transformer operating at arbitrary dual band is proposed in [5] by Wu. In [6], a modified shunt-stub dual-band impedance transformer was used to achieve matching a load with different complex impedances at two frequencies to a real impedance source by Chuang. Wu et al. discusses the situation where both source and load impedances are complex and frequency dependent in [7]. Recently, many novel matching techniques have been proposed to improve the performance of the dual-band matching [8–14]. However, these existing dual-band matching techniques in [1–14] can not realize dual-band matching at two relatively closed operating frequencies ( $n = f_2/f_1 \leq 1.2$ ) in a small circuit area because of their complex structure. Besides, The application of coupled-line was extensively investigated recently [15–21].

In the light of these issues, this paper presents a new dual-band matching technique, which uses the dual-band coupled-line transformer approach. The proposed dual-band matching technique can realize matching arbitrary complex impedance to arbitrary complex impedance at any two arbitrary frequencies, as well as at two relatively closed operating frequencies ( $n = f_2/f_1 \leq 1.2$ ), and occupy a very small circuit area. The proposed design methodology requires the use of a novel dual-band impedance transformer, which has different electronic length at two operating frequencies. This transformer ingenious uses the characteristics of coupled-line in a unique way to realize dual-band complex impedance matching. To the best of the authors' knowledge, this circuit has never been used explicitly to realize a dual-band impedance transformer with two different complex impedances at two different operating frequencies.

It is very interesting that this novel dual-band transformer can also be used in dual-band passive circuit design. This paper focuses on using the proposed transformer to transform  $50\ \Omega$  impedance to the ideal load impedances of the transistor at two frequency bands. To validate the proposed methodology, the matching circuits are designed to match  $50\ \Omega$  to the ideal load impedances obtained from source-pull and load-pull data of a 30 W gallium nitride (GaN)-based device (CGH27030 in Cree [22]) using Agilent's Advanced Design System at two designed frequency simultaneously. These matching circuits are further used in the design of 30 W dual-band class-AB PA for Global System for Mobile

Communications (GSM) and Wideband Code Division Multiple Access (WCDMA) at 1800 and 2140 MHz, respectively.

## 2. DESIGN METHODOLOGY

As shown in Figure 1, this matching network configuration is fundamentally based on extending the single-band coupled-line transformer, which is an arbitrary complex impedance transformer from [23], to dual-band application.

In this design, the key element of this network is a coupled-line attached with two dual-band/dual-susceptance parts at its across terminals. The coupled-line has even- and odd-mode characteristic impedances  $Z_{0e}$ ,  $Z_{0o}$  and electrical length  $\theta_1$  at the first band center frequency,  $f_1$ . Then, it has corresponding even- and odd-mode characteristic impedances  $Z_{0e}$  and  $Z_{0o}$ , and electrical length  $\theta_2$  at the second band center frequency  $f_2$ . The two dual-band/dual-susceptance parts present two different susceptances  $jX_{T11}$ ,  $jX_{T12}$  and  $jX_{T21}$ ,  $jX_{T22}$  at  $f_1$  and  $f_2$ , respectively. Due to these dual-band operating characteristic, the proposed dual-band matching network can realize an impedance transformation from  $Z_L$  to two arbitrary complex impedances,  $Z_{in1}$  and  $Z_{in2}$  at  $f_1$  and  $f_2$ , respectively. The methodology will be explained in the following section.

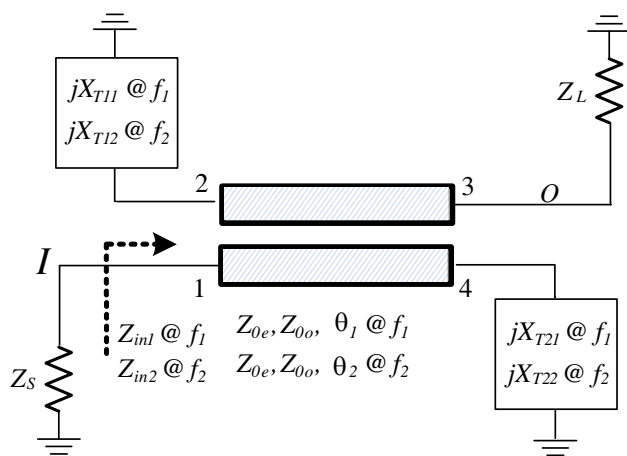


**Figure 1.** The circuit model of the proposed dual-band matching network.

### 2.1. Coupled-line Transformer

At each operate frequency, the proposed dual-band coupled-line impedance transformer can be equivalent to a single-band coupled-line impedance transformer. The single-band coupled-line impedance transformer has been analyzed in [23]. Figure 2 shows the generalized circuit configuration of the proposed single-band coupled-line impedance transformer. It consists of an arbitrary-length coupled-line section ( $Z_{0e}, Z_{0o}, \theta$ ) and two reactive elements ( $jX_{T1}, jX_{T2}$ ). Five design parameters ( $Z_{0e}, Z_{0o}, \theta, jX_{T1}, jX_{T2}$ ) exist in this proposed matching structure, resulting in the wide range of matched source and load impedances ( $Z_S = R_S + jX_S, Z_L = R_L + jX_L$ ), various available solutions, and a compact size.

If the values of  $Z_{0e}, Z_{0o}, \theta$  are manually determined, other two parameters  $jX_{T1}, jX_{T2}$  can be calculated by closed-form equations. The analytical design expressions, and the achieved results are

$$\begin{cases} X_{T1} = \frac{C_1 + C_3 + \sqrt{2C_2}}{C_4}, \\ X_{T2} = \frac{C_5 + C_6 + \sqrt{2C_2}}{C_7}, \end{cases} \quad (1a)$$

$$\begin{cases} X_{T1} = \frac{C_1 + C_3 - \sqrt{2C_2}}{C_4}, \\ X_{T2} = \frac{C_5 + C_6 - \sqrt{2C_2}}{C_7}, \end{cases} \quad (1b)$$

where  $C_1$ – $C_7$  were interim parameters calculated from  $Z_{0e}, Z_{0o}, \theta, Z_S, Z_L$  [23]. The values of  $Z_{0e}, Z_{0o}, \theta$  can be freely chosen when  $C_2 \geq 0$  is satisfied.

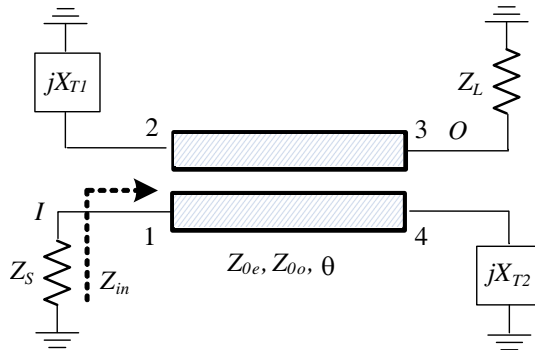


**Figure 2.** The circuit model of the single-band coupled-line impedance transformer from [23].

To make this coupled-line transformer satisfy dual-band application requirements, these parameters should be considered in two frequency bands. When the parameters  $Z_{0e}$ ,  $Z_{0o}$ ,  $\theta_1$  are determined at the first frequency  $f_1$ , these parameters are turned to be  $Z_{0e}$ ,  $Z_{0o}$ ,  $\theta_2 = n\theta_1 (n = f_2/f_1)$  at the second frequency  $f_2$ . After that, the parameters  $X_{T1}$ ,  $X_{T2}$  can also be calculated by closed-form Equations (1a) and (1b) at  $f_1$  and  $f_2$  when the design equations in [23] are considered. In respect to that the total calculation is based on analytical formulas, and the design theory of the proposed coupled-line transformer is direct and accurate.

### 2.2. Dual-band/Dual-susceptance Stub

The next step in the matching network design is to obtain the calculated parameters  $X_{T1}$ ,  $X_{T2}$  by using dual-band/dual-susceptance stubs, as shown in Figure 3.

The dual-band/dual-susceptance stub is realized by open-circuit transmission line  $T_1$  or short-circuit transmission line  $T_2$ . Each of them has its own electronic length at two different operating frequencies, so that they can present different susceptances at two different operating frequencies seen into from point  $A$ . The choice of using either open-circuit line or short-circuit line in order to realize dual-band/dual-susceptance stub depends on the realization of it with a minimum stub length.

To satisfy the demand of the dual-band coupled-line impedance transformer, the result of the first dual-band/dual-susceptance stub should be as follows:

$$\begin{cases} Z_{T1}(f_1) = jX_1 = jX_{T11} & @f_1 \\ Z_{T1}(f_2) = jX_2 = jX_{T12} & @f_2 \end{cases}, \quad (2a)$$

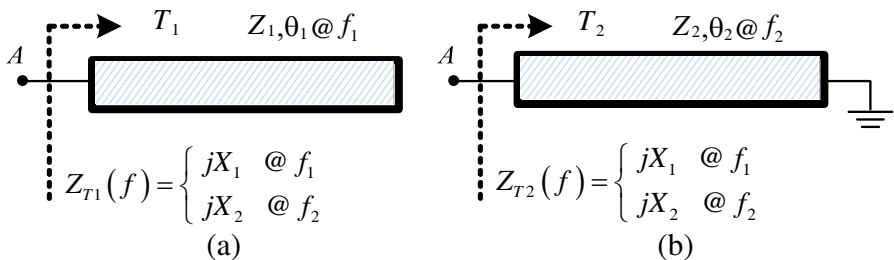


**Figure 3.** Proposed dual-band/dual-susceptance stub. (a) Open-circuit, (b) short-circuit.

And the second dual-band/dual-susceptance stub should be as follows:

$$\begin{cases} Z_{T2}(f_1) = jX_1 = jX_{T21} & @f_1 \\ Z_{T2}(f_2) = jX_2 = jX_{T22} & @f_2 \end{cases} \quad (2b)$$

where  $X_1$ ,  $X_2$  can be positive or negative, depending on the required susceptance value calculated from (1a) and (1b).  $X_{T11}$ ,  $X_{T12}$ ,  $X_{T21}$ ,  $X_{T22}$  are the calculated parameters shown in Figure 1. In the following subsection, the use of the open-circuit transmission line and short-circuit transmission line for the design of such a dual-band/dual-susceptance stub are discussed.

$T_1$  is an open-circuit transmission line which has characteristic impedance  $Z_1$  and electrical length  $\theta_1$  at the first frequency. The impedance of the open-circuit transmission line seen into from point  $A$  can be obtained by transmission line impedance equation as follow [24]:

$$Z_{T1}(f_1) = -jZ_1 \cot \theta_1 \quad @f_1. \quad (3)$$

when it works at the second operating frequency  $f_2$ , it has the same characteristic impedance  $Z_1$  and physical length with the situation of it works at the first operating frequency  $f_1$ . Thus, the impedance of the open-circuit transmission line seen into from point  $A$  at the second operating frequency turned to be:

$$Z_{T1}(f_2) = -jZ_1 \cot n\theta_1 \quad @f_2, \quad (4)$$

where  $n$  is the frequency ratio  $n = f_2/f_1$  greater than 1. Thus, the main goal is to obtain the design parameters  $Z_1$  and  $\theta_1$  as illustrated in Figure 3(a). Equations (3) and (4) can be solved simultaneously using graphical methods or numerical techniques to obtain the values of  $Z_1$  and  $\theta_1$ . The obtained value of  $\theta_1$  is assumed at  $f_1$ , furthermore we can use it to calculate the physical length of the open-circuit transmission line. Once these parameters for the open-circuit transmission line are known, the design parameters for the dual-band/dual-susceptance stub can be easily determined.

In the same way, the design parameters for the short-circuit transmission line  $T_2$  can be determined from the following equations:

$$Z_{T2}(f_1) = jZ_2 \tan \theta_2 \quad @f_1, \quad (5)$$

$$Z_{T2}(f_2) = jZ_2 \tan n\theta_2 \quad @f_2. \quad (6)$$

The last step of the dual-band coupled-line impedance transformer design is attaching two dual-band/dual-susceptance stubs to the two across ports of coupled-line, as shown in Figure 4. When the two cross-ports of coupled-line have corresponding reactive load at the two operating frequencies, the remaining two ports will realize the required impedance transformation from  $Z_L$  to  $Z_{in1}@f_1$  and  $Z_{in2}@f_2$ . After that, the required dual-band impedance matching network can be implemented finally.

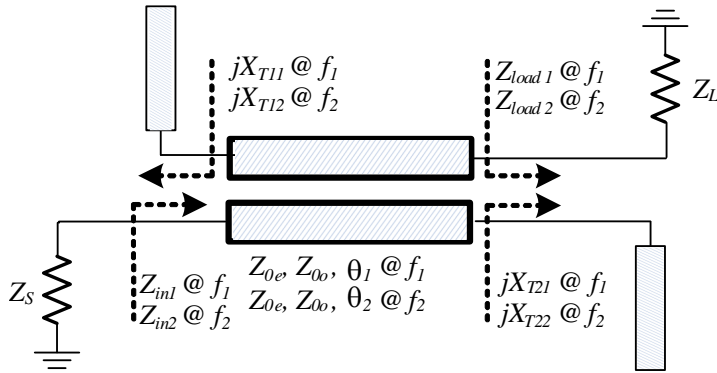


Figure 4. Proposed dual-band matching network.

Table 1. Source-pull and load-pull results.

Impedance/ $\Omega$	$f_1$	$f_2$
Source-pull impedance	$6.3 + j*7.7$	$3.9 - j*1.3$
Load-pull impedance	$10.8 + j*6.7$	$7.3 - j*1.2$
Desired input impedance	$8.613 + j*1.030$	$7.277 + j*19.930$
Desired output impedance	$12.878 + j*5 \cdot 190$	$12.132 + j*20.903$

### 3. EXPERIMENT

Based on the proposed methodology, a dual-band matching circuit is realized for matching specific complex impedances to a  $50 \Omega$  load. The values of the complex impedances to be matched are obtained from the source-pull and load-pull analysis of a stabilized GaN based device (CGH27030 from Cree), which is biased at a drain voltage and current of 28 V and 150 mA, respectively, as listed in Table 1. The source-pull and load-pull data are based on obtaining optimal PAE at the two frequencies of 1800 MHz and 2140 MHz. The design methodology of dual-band matching network is validated by designing input and output matching networks for a class-AB power amplifier.

#### 3.1. Matching Network Design

For presenting the ideal source and load impedance to the transistor, the coupled-line impedance transformers need to match  $50 \Omega$  load to the desired impedances listed in Table 1. The input and output matching circuits are designed on a Rogers' RO4350B substrate which has a dielectric constant of 3.48, a substrate thickness of 0.76 mm and a tangent of dielectric loss angle of 0.003.

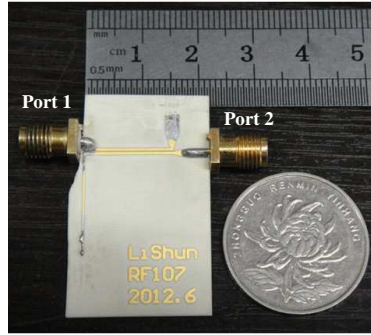


**Figure 5.** Photograph of the fabricated example.

**Table 2.** Design parameters for input and output dual-band coupled-line impedance transformers.

Proposed Transformer	$Z_{0e}$	$Z_{0o}$	$\theta_1@f_1$	$\theta_2@f_2$	$X_{T11}$	$X_{T12}$	$X_{T21}$	$X_{T22}$
Input Match	120 $\Omega$	50 $\Omega$	41°	48.74°	-64.67	-48.42	-38.17	-13.43
Output Match	120 $\Omega$	50 $\Omega$	48°	57.07°	-76.29	-61.75	-66.10	-39.58

The input matching circuit and the output matching circuit are designed in the same way. Therefore, in this paper, we only discuss and test the output matching circuit as an example to show the performance of the proposed dual-band matching structure. The size of the whole output matching circuit is 22 mm  $\times$  25 mm and the photograph of it is shown in Figure 5.

Table 2 list the numerically obtained design parameters of the input and output dual-band coupled-line impedance transformers. Table 3 lists the numerically obtained design parameters for all dual-band/dual-susceptance stubs. Table 4 represents the physical design parameters for the fabricated dual-band power amplifier including stabilized circuit, input- and output-matching networks corresponding to the numerically calculated design parameters reported in Tables 2 and 3. An optimization of the physical design parameters is done to compensate for the effects of discontinuities. The slight optimization is evaluated in Agilent's Advanced Design System used as circuit simulator, and the optimized results are listed in Table 4 compare with the calculated results.

**Table 3.** Design parameters for input and output dual-band/dual-susceptance stubs.

Dual-band/dual-susceptance stub	$Z_0$	$\theta_1@f_1$	$\theta_2@f_2$
Input Match stub 1	61.46 $\Omega$	43.54°	51.76°
Input Match stub 2	101.25 $\Omega$	69.32°	82.41°
Output Match stub 1	40.81 $\Omega$	28.13°	33.44°
Output Match stub 2	110.63 $\Omega$	59.13°	70.30°

**Table 4.** Physical design parameters for proposed dual-band power amplifier.

Parameters	Calculated	Optimized	Parameters	Calculated	Optimized
$T_1$	W=1.18 mm L=12.41 mm	W=1.18 mm L=11.71 mm	$T_4, T_5$	W=1.68 mm L=23.08 mm	W=1.68 mm L=23.08 mm
$CL_1$	W=0.52 mm S=0.17 mm L=12.35 mm	W=0.52 mm S=0.17 mm L=12.35 mm	$C_3, C_5$	Murata ERB21B5C2E8R 2DDX1; C=8.2 pF	Murata ERB21B5C2E8R 2DDX1; C=8.2 pF
$T_2$	W=0.38 mm L=20.54 mm	W=0.38 mm L=20.34 mm	$C_4, C_6$	Murata ERB21B5C2E150 JDX1; C=15 pF	Murata ERB21B5C2E150 JDX1; C=15 pF
$C_1$	Murata ERB21B5C2E3R 9CDX1; C=3.9 pF	Murata ERB21B5C2E3R 9CDX1; C=3.9 pF	$T_6$	W=1.68 mm L=4.49 mm	W=1.68 mm L=4.29 mm
$T_3$	W=1.68 mm L=3.79 mm	W=1.68 mm L=3.49 mm	$C_7$	Murata ERB21B5C2E3R 6CDX1; C=3.6p	Murata ERB21B5C2E3R 6CDX1; C=3.6p
$R_1$	CR05-101J 100 $\Omega$	CR05-101J 100 $\Omega$	$T_7$	W=0.29 mm L=17.65 mm	W=0.29 mm L=17.44 mm
$C_2$	Murata GRM1885C1H3R 0CZ01; C=3 pF	Murata GRM1885C1H3R 0CZ01; C=3 pF	$CL_2$	W=0.52mm S=0.17 mm L=14.46 mm	W=0.52 mm S=0.17 mm L=14.46 mm
$R_2$	CR05-470J 47 $\Omega$	R05-470J 47 $\Omega$	$T_8$	W=2.31 mm L=7.79 mm	W=2.31 mm L=7.58 mm

### 3.2. Dual-band Class-AB Power Amplifier Design

Based on the above designed matching network, a 30 W class-AB power amplifier has been designed to verify the performance of the proposed coupled-line transformer in the application of high power active circuits. The architecture of the proposed dual-band power amplifier is shown in Figure 6.

There are two more works need to do in the design of the proposed amplifier: biasing and stabilizing the transistor. The quarter-wave

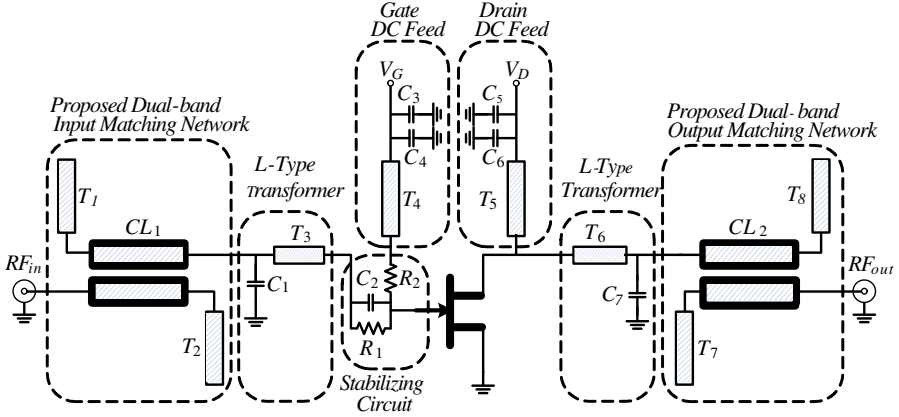


**Figure 6.** Architecture of the proposed dual-band power amplifier.

short circuited stub (SCSS) has the advantage of being an open circuit at the fundamental, and presents a short circuit at successive even harmonics. It can additionally provide a convenient bias insertion point, if the RF short is made using a suitable bypass capacitor [25]. So a short-circuit quarter-wave transmission line which is calculated at the middle frequency of  $f_1$  and  $f_2$  has been used in the present application as DC feed. The characteristic impedance of this quarter-wave transmission line is chosen as  $50\ \Omega$  and the short-circuit is realized by two capacitances which resonates at  $f_1$  and  $f_2$ , respectively. The transistor is stabilized using paralleled resistance and capacitance at its input and a resistance at its gate DC feed circuit.

When use the dual-band coupled-line transformer to match the load-pull impedance to  $50\ \Omega$  directly, output matching network results in high-impedance lines which is difficult to realize accurately with the authors' fabrication facility. As a result, we add an L-type transformer to transform the load-pull impedance to intermediate impedance which is easy to realize accurately with the authors' fabrication facility, as listed in Table 1.

The corresponding physical design parameters of the amplifier are listed in Table 4. Make the appropriate adjustments of the direction of these transmission lines in the circuit to avoid unwanted coupling between them and obtain a smaller circuit size. The size of the input- and output-matching networks are  $26\ \text{mm} \times 30\ \text{mm}$  and  $26\ \text{mm} \times 24\ \text{mm}$ , respectively. Matching circuit is the largest part of the power amplifier module, so the miniaturization of the matching circuit can greatly reduce the size of the power amplifier module. The overall size of the designed class-AB PA is  $63\ \text{mm} \times 57\ \text{mm}$ . If the DC feed transmission

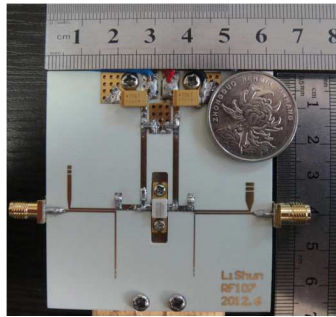


**Figure 7.** Photograph of the fabricated dual-band power amplifier.

line layout in a bend way, the size of the PA will be reduced to  $63\text{ mm} \times 30\text{ mm}$ . The photograph of the fabricated dual-band power amplifier is shown in Figure 7.

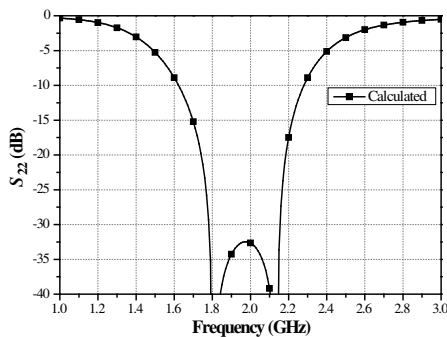
## 4. RESULTS AND DISCUSSION

To validate the matching capability of the designed matching network, we terminate it with a  $50\ \Omega$  impedance load and measure another port's return loss and test the performance of the dual-band PA which is matched by the proposed matching network. The calibrated vector network analyzer Agilent E5071C PNA-L Network Analyzer was used to test the frequency responses of them.

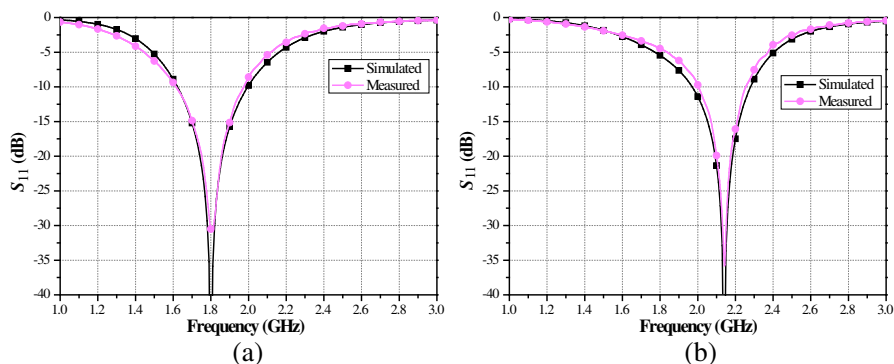
### 4.1. Matching Network

Figure 8 shows the calculated results of the proposed dual-band coupled-line impedance transformer's reflection coefficient magnitudes at Port 2 when Port 1 terminated with a fictitious load which has different impedance at the two frequency bands. As shown in Figure 8, the proposed impedance transformer can accurately match two different complex impedances at two designed frequency simultaneously and has 20% and 15% bandwidth for which the reflection coefficient magnitudes are less than 0.1, respectively.

Figure 9(a) shows the simulated and measured results of the fabricated matching networks which is shown in Figure 5 at the first frequency 1800 MHz. To demonstrate the performance of the fabricated matching network, the  $s$ -parameters data plotted in Figure 9 have been equivalent to terminate the Port 1 with  $(12.878 - j*5.190)\ \Omega$  load which is the conjugate of the complex impedance as the network designed to present at the first frequency 1800 MHz. Therefore,



**Figure 8.** Calculated result of the proposed dual-band coupled-line impedance transformer.



**Figure 9.** Simulated and measured performance of the fabricated examples: (a) at 1800 MHz, (b) at 2140 MHz.

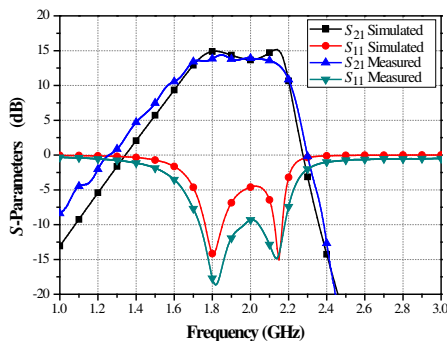


**Figure 10.** Simulated and measured  $S$ -parameters of the proposed dual-band power amplifier.

**Table 5.** Comparison with the current state of the art.

Methodology	Matching rang	Performance return loss	Experiment	Size of the matching network	PA design	Reference no.
Dual-ban Chebyshey transformer	Same real impedance to same real impedance	RL<-20 dB for $\pm 75$ MHz @ $f_1, f_2$	No	N/A	No	[1]
Dual-ban unequal stepped impedance transformer	Arbitrary complex impedances to arbitrary complex impedance	RL<-20 dB for $\pm 50$ MHz @ $f_1, f_2$	No	N/A	No	[3]
Three-section step-impedance transformer	Arbitrary complex impedances to same real impedance	RL<-20 dBfor $\pm 50$ MHz @ $f_1, f_2$	No	N/A	No	[4]
Step-impedance transformer with two-section stubs	Arbitrary complex impedances to same real impedance	RL<-15 dB for $\pm 70$ MHz @ $f_1, f_2$	Yes	76 mm $\times$ 10 mm	No	[6]
Dual-band multi-section step-impedance transformer	Arbitrary real impedances to arbitrary real impedance	RL<-20 dBfor $\pm 200$ MHz @ $f_1, f_2$	Yes	111 mm $\times$ 18 mm	No	[7]
Dual-band/dual-characteristic impedance transformer	Arbitrary complex impedances to same real impedance	RL<-15 dBfor $\pm 10$ MHz @ $f_1, f_2$	Yes	74 mm $\times$ 75 mm	Yes	[8]
T-section dual-band impedance transformer	Arbitrary complex impedances to same real impedance	RL<-10 dBfor $\pm 90$ MHz @ $f_1, f_2$	No	N/A	No	[9]
Using resonators with microstrip lines	Arbitrary complex impedances to same real impedance	Not given	Yes	20 mm $\times$ 50 mm	Yes	[10]
Dual-Band coupled-line impedance transformer	Arbitrary complex impedance to arbitrary complex impedance	RL<-10 dBfor $\pm 200$ MHz @ $f_1$ RL<-10 dB for $\pm 150$ MHz @ $f_2$	Yes	22 mm $\times$ 25 mm	Yes	This work

the matching capability and bandwidth of the matching network is easy to evaluate in this figure. As shown in Figure 9(a), the proposed impedance transformer can accurately match the complex impedance at the designed frequency and has 20% bandwidth for which the reflection coefficient magnitudes are less than 0.1. Because the transformer is not designed to transform the load to  $(12.878 + j*5.190) \Omega$  at 2140 MHz, the reflection coefficient magnitude is not small at 2140 MHz. In the same way, Figure 9(b) shows the simulated and measured results of the fabricated matching networks which is shown in Figure 5 at the second frequency 2140 MHz. One can also find the deviation between the measured and simulated results is small and that approved the validity of the proposed matching technique. This matching circuit is then used in designing a class-AB Power Amplifier.

#### 4.2. Dual-band Class-AB Power Amplifier Design

The bias point of the power amplifier is  $V_{DS} = 28$  V and  $I_{DS} = 150$  mA at a Class-AB operation. Figure 10 shows the simulated and measured

frequency responses of the fabricated dual-band PA based on small signal  $S$ -parameters. As shown in Figure 10, the dual-band PA achieves a power gain exceeding 13.5 dB and 12.5 dB in the 1800 MHz and 2140 MHz operation bands, respectively. The PA has a 1-dB transmission bandwidth of 420 MHz and 70 MHz in the 1800 MHz and 2140 MHz operation bands, respectively. These bandwidths of the PA can satisfy the requirement of base stations in the GSM 1800 and WCDMA concurrent communication systems. Finally, they indicated that the matching conditions of the input and output terminals are good for both of the desired bands.

The comparative perspective of the present work in light with the existing state of the art is presented in Table 5.

## 5. CONCLUSION

A miniaturized and novel dual-band impedance transformer based on single coupled-line section has been proposed. The rigorous analysis of the corresponding closed-form design equations are given in this paper. Furthermore, fabricated transformer examples with good simulated and measured results verify the proposed structure and its design method. Finally, a novel miniaturized dual-band power amplifier by using this new dual-band impedance matching technique is designed, fabricated and demonstrated. As a result, this proposed dual-band matching technique with an analytical design approach provides a miniaturized matching method with inherent DC-block function for the design of dual-band components and systems.

## ACKNOWLEDGMENT

This work was supported in part by the National Natural Science Foundation of China (No. 61001060, No. 61201025, and No. 61201027), the Fundamental Research Funds for the Central Universities (No. 2012RC0301), and Important National Science & Technology Specific Projects (No. 2010ZX03007-003-04).

## REFERENCES

1. Orfanidis, S. J., "A two-section dual-band Chebyshev impedance transformer," *IEEE Microwave and Wireless Components Letters*, Vol. 13, No. 9, 382–384, 2003.
2. Monzon, C., "A small dual-frequency transformer in two sections," *IEEE Transactions on Microwave Theory and Techniques*, Vol. 51, No. 4, 1157–1161, 2003.

3. Wu, Y., Y. Liu, and S. Li, "A dual-frequency transformer for complex impedances with two unequal sections," *IEEE Microwave and Wireless Components Letters*, Vol. 19, No. 2, 77–79, 2009.
4. Liu, X., Y. Liu, S. Li, F. Wu, and Y. Wu, "A three-section dual-band transformer for frequency-dependent complex load impedance," *IEEE Microwave and Wireless Components Letters*, Vol. 19, No. 10, 611–613, 2009.
5. Wu, Y., Y. Liu, and S. Li, "A compact pi-structure dual band transformer," *Progress In Electromagnetics Research*, Vol. 88, 121–134, 2008.
6. Chuang, M.-L., "Dual-band impedance transformer using two-section shunt stubs," *IEEE Transactions on Microwave Theory and Techniques*, Vol. 58, No. 5, 1257–1263, 2010.
7. Wu, Y., Y. Liu, S. Li, C. Yu, and X. Liu, "A generalized dual-frequency transformer for two arbitrary complex frequency-dependent impedances," *IEEE Microwave and Wireless Components Letters*, Vol. 19, No. 12, 792–794, 2009.
8. Rawat, K. and F. M. Ghannouchi, "Dual-band matching technique based on dual-characteristic impedance transformers for dual-band power amplifiers design," *IET Microwaves, Antennas & Propagation*, Vol. 5, No. 14, 1720–1729, 2011.
9. Nikravan, M. A. and Z. Atlasbaf, "T-section dual-band impedance transformer for frequency-dependent complex impedance loads," *Electronics Letters*, Vol. 47, No. 9, 551–553, 2011.
10. Wang, Z. and C. Park, "Dual-band GaN HEMT power amplifier using resonators in matching networks," *2011 IEEE 12th Annual Wireless and Microwave Technology Conference (WAMICON)*, 1–4, 2011.
11. Jimenez-Martin, J. L., V. Gonzalez-Posadas, J. E. Gonzalez-Garcia, F. J. Arques-Orobon, L. E. Garcia-Munoz, and D. Segovia-Vargas, "Dual band high efficiency class ce power amplifier based on CRLH diplexer," *Progress In Electromagnetics Research*, Vol. 97, 217–240, 2009.
12. Castaldi, G., V. Fiumara, and I. Gallina, "An exact synthesis method for dual-band Chebyshev impedance transformers," *Progress In Electromagnetics Research*, Vol. 86, 305–319, 2008.
13. Fukuda, A., H. Okazaki, S. Narahashi, and T. Nojima, "Concurrent multi-band power amplifier employing multi-section impedance transformer," *2011 IEEE Topical Conference on Power Amplifiers for Wireless and Radio Applications (PAWR)*, 37–40, 2011.

14. Ciccognani, W., E. Limiti, and L. Scucchia, "A new structure for the design of dual band power amplifiers," *2011 Workshop on Integrated Nonlinear Microwave and Millimetre-wave Circuits (INMMIC)*, 1–4, 2011.
15. Ye, C.-S., Y.-K. Su, M.-H. Weng, C.-Y. Hung, and R.-Y. Yang, "Design of the compact parallel-coupled lines wideband bandpass filters using image parameter method," *Progress In Electromagnetics Research*, Vol. 100, 153–173, 2010.
16. Wu, Y. and Y. Liu, "An unequal coupled-line Wilkinson power divider for arbitrary terminated impedances," *Progress In Electromagnetics Research*, Vol. 117, 181–194, 2011.
17. Wong, Y. S., S. Y. Zheng, and W. S. Chan, "Multifolded bandwidth branch line coupler with filtering characteristic using coupled port feeding," *Progress In Electromagnetics Research*, Vol. 118, 17–35, 2011.
18. Wu, Y. and Y. Liu, "A coupled-line band-stop filter with three-section transmission-line stubs and wide upper pass-band performance," *Progress In Electromagnetics Research*, Vol. 119, 407–421, 2011.
19. Kuo, J.-T., C.-Y. Fan, and S.-C. Tang, "Dual-wideband bandpass filters with extended stopband based on coupled-line and coupled three-line resonators," *Progress In Electromagnetics Research*, Vol. 124, 1–15, 2012.
20. Li, B., X. Wu, N. Yang, and W. Wu, "Dual-band equal/unequal Wilkinson power dividers based on coupled-line section with short-circuited stub," *Progress In Electromagnetics Research*, Vol. 111, 163–178, 2011.
21. Lin, Z. and Q.-X. Chu, "A novel approach to the design of dual-band power divider with variable power dividing ratio based on coupled-lines," *Progress In Electromagnetics Research*, Vol. 103, 271–284, 2010.
22. Cree, "CGH27030 GaN HEMT for linear communications ranging from VHF to 3 GHz," Rev. 3.5, 2011.
23. Wu, Y., Y. Liu, S. Li, and S. Li, "A novel high-power amplifier using a generalized coupled-line transformer with inherent DC-block function," *Progress In Electromagnetics Research*, Vol. 119, 171–190, 2011.
24. Pozar, D. M., *Microwave Engineering*, 3rd Edition, John Wiley & Sons, Inc., 2005.
25. Steve, C. C., *RF Power Amplifiers for Wireless Communications*, 2nd Edition, 103–104, Artech House, Inc., 2006.